Hydrodynamic Drag Force Acting upon a Spherical Particle on a Rough Bed Composed of Identical Particles

By Hiroji NAKAGAWA and Tetsuro TSUJIMOTO

(Manuscript received January 16, 1981)

Abstract

In order to investigate the characteristics of drag force acting upon a spherical particle near a rough bed, a measuring instrument was devised by making use of strain gauges and a dynamic strain-meter. The measurements of drag force were conducted under various conditions where the relative exposure of a particle to the flow and the constitution of surrounding particles were changed. These effects on drag force acting upon a particle near a bed were clarified experimentally. Not only the average magnitude of drag force but also the statistical properties of its fluctuation were investigated. The results obtained by these measurements and their analyses must be made available for the research study of mechanics of bed load transport.

1. Introduction

Although hydrodynamic forces acting upon sand grains on a bed as well as their fluctuations must be precisely evaluated in order to clarify the mechanism of bed load transport, the previous investigations leave much to be solved because these forces are complicatedly connected with not only the characteristics of turbulent shear flow near the bed but also the orientations and interferences of individual bed materials and it is not easy to measure them systematically in flowing water. Hence, only a few studies have been conducted about hydrodynamic forces. On the other hand, the aerodynamic forces acting upon a particle are comparatively easy to measure, and they have been earnestly inspected by Chepil[1),2),3)] and others.

As for the hydrodynamic forces acting upon bed materials, Coleman[4),5)] and Aksoy[6)] measured the drag force under some idealized conditions, and Davies and Samad[7)] devised a method to measure the lift force acting upon a particle along a rough bed. These are recognized as a kind of direct measurements. On the other hand, Garde and Sethuraman[8)] evaluated an apparent drag coefficient indirectly for a spherical particle rolling along a bed. This approach is something instructive but has some weak points. One of them is that some contributions on the measured apparent drag coefficient cannot be separated each other.

In addition to them, Bagnold[9)] and Coleman[10)] have recently eagerly investigated

the hydrodynamic force connected with bed load transport problem. However, their experimental data have not always been adequately arranged so as to obtain any definite conclusion which can be applied to any sediment transport model, and we can say that this problem is still now important to tackle with.

Furthermore, neither the effect of exposure of a particle to flow nor the interference effect by surrounding particles on the bed were investigated in the previous studies, despite the fact that these effects are very important for clarifying the mechanics of bed load movements; not only incipient motion but also travelling process along the bed. Therefore, on evaluating the hydrodynamic forces in bed load transport problem, the drag or lift coefficient has inevitably been assumed only by consulting the empirical value for free falling particle in still liquid.

Considering the above state of investigations, the authors devised an equipment to measure a drag force dynamically by using some strian gauges and a dynamic strainmeter, and investigated the characteristcs of drag force acting upon a particle on a stream bed, which may be more dominant particularly for bed load transport rather than those of lift force. In this study, not only the mean drag coefficient but also the effect of relative exposure of the particle above the bed and mutual interference by surrounding particles on the bed are investigated. Of course, the characteristcs of lift force and others must be investigated in the future in order to obtain more detailed recognition or more rigorous description of sediment transport process.

2. Experimental Equipment and Procedures of Measurements

The equipment devised to measure a drag force acting upon a particle near a bed is shown in **Fig. 1-(a)**, and this is a cantilever-strain-gauge type. A testing spherical particle made of brass of 1.9cm is fixed on the top of an acrylic rod which has a rectangular section of $1\text{cm}\times 0.6\text{cm}$; the lower end of this rod is fastened by a heavy pedestal made of brass, the height of which is adjustable by four screws which change the exposure of the testing particle to flow, as shown in **Fig. 1-(a)** The elasticity modulus of the acrylic rod is $2.794\times 10^9\text{N/m}^2$. Near the lower end of this rod, four

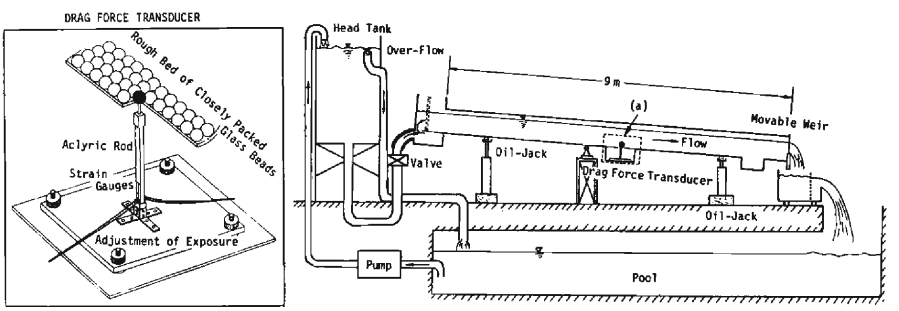

(a) (b)

Fig. 1 Experimental equipment.

sheets of strain gauges were stuck by a way devised so as to remove the effect of lift force. These strain gauges are for the use of plastic materials and protected by a kind of coating agent against water. The four strain gauges acted as kind of bridge circuits and were connected with a dynamic strain-meter. The out-put of this system was registered by a digital recorder through a low-pass-filter. The equipment explained above was set in the tilting flume 9m long, 33cm wide and 33cm deep, as shown in **Fig. 1-(b)**.

Before a series of measurements, the relationship between the out-put of the instrument and the known load force acting upon a testing particle was inspected to learn the calibration constant C_{VD}(gf/volt; 1gf=0.098N), in the manner shown in **Fig. 2-(a)**. The result of this calibration is shown in **Fig. 2-(b)**, and a linear relationship is sufficiently evident from this figure.

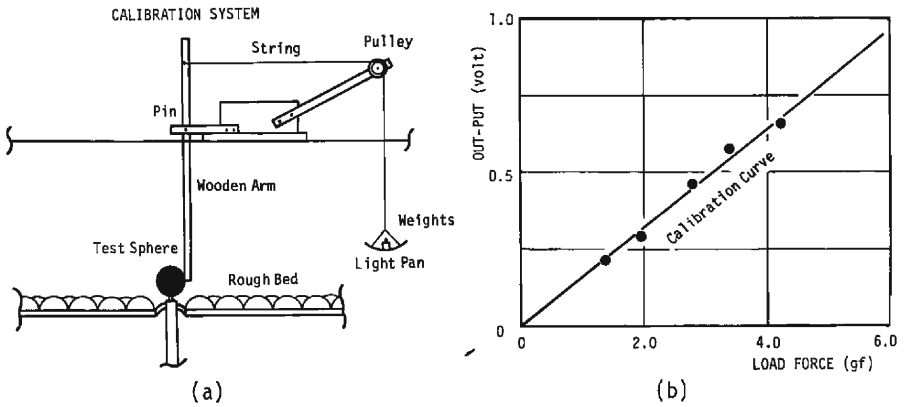

Fig. 2 Calibration of measuring equipment.

After setting the testing particle under pre-determined conditions, water flow was induced gradually so as to prevent a heavy load from acting upon the particle rapidly. As soon as the flow condition reached the pre-determined setting, the measurement was started. The period of measurement was 5min., and the data were registered every 0.5sec. Before and after the measurement of drag force, the water surface elevation along the flume and the vertical velocity profile were measured by a point gauge and a current meter of a propeller type the diameter of wihch was 0.5cm.

The registered data was calibrated and analyzed statistically by an electronic computer. On the calculation of the spectra, some consideration of a response function for the instrument of measurement is necessary. If the system of the measurement is linear, the filter $H(f)$ can be given by

$$H(f)=|1-(f/f_0)| \tag{1}$$

$$2\pi f_0=\sqrt{k/M} \tag{2}$$

where f_0 is an eigen-frequency of the measurement system, k is the spring constant of the acryilc rod, and M is the virtual mass of the testing particle. The power spectral

density of drag force $P_{DD}(f)$ [gf² sec] can be related to that of the out-put $P_{VV}(f)$ [volt² sec] using the above obtained response function $H(f)$, as follows;

$$P_{DD}(f)=C_{DV}^2\cdot H(f)\cdot P_{VV}(f) \tag{3}$$

By the way, because the range of frequency to be analyzed here is lower than 1Hz and f_0 is about 50Hz in the case of this measurement sestem, $H(f)$ is about unity after Eq. (1). The spectra were calculated by the maximum entropy method (M. E. M.) by which stable spectra can be favorably obtained even if the number of data are small.

As an additional remark, the friction velocity was calculated by using the energy gradient I_e which was obtained by the following equation.

$$I_e=i_w-Fr^2(i_w-i_b) \tag{4}$$

where Fr is the Froude number, i_w is the slope of water surface and i_b is the bed slope. The calculated friction velocity was verified by the measurement of flow velocity, based on the logarithmic law for rough turbulent regime.

3. Characteristics of Drag Force Acting upon a Solitary Particle on a Rough Bed

A bed was composed of glass beads of which diameter was about same as that of the testing particle, and they were arranged on the bed of the flume in the closest possible packing. The height of the testing particle over the bed was adjusted by the four screws of the pedestal, and the measurements were conducted under nine sets of conditions of the relative exposure from 0 to 1.0. Here, the relative exposure represents the dimensionless exposure of the testing particle to flow and is defined as

$$H_{e*}=H_e/d \tag{5}$$

where H_e is the quantity indicated in **Fig.3** and d is diameter of the testing particle. The conditions and the results of the experiments are shown in **Table 1**. In **Table 1**, D is the time-averaged magnitude of drag force, and α_D, Sk and Kr are its variation coefficient, skewness and kurtosis, respectively.

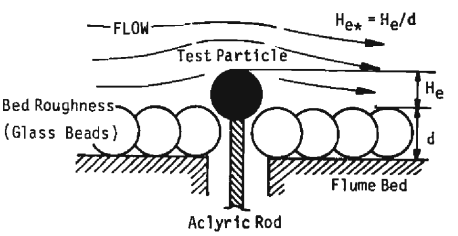

Fig. 3 Definition sketch.

In **Fig. 4-(a)** is shown the relationship between the time-averaged magnitude of drag force D and the friction velocity u_* obtained by the experiments with a parameter H_{e*}. Accoring to this figure, a linear relation is recognized between D and u_*^2 with

Table 1 Experimental conditions and results (solitary particle).

Case	H_e/d	Run	u_*d/ν	h/d	D(gf)	$D/\rho u_*^2 d^2$	α_D	Sk	Kr
1	1.00	Y-12	239	2.74	0.252	43.09	0.367	0.561	3.122
		Y-13	429	3.87	0.439	23.33	0.353	0.576	2.949
		Y-10	593	5.68	0.603	16.82	0.265	0.557	3.627
		Y-14	612	4.94	0.681	17.83	0.333	0.940	3.709
		Y-15	637	5.13	0.828	20.03	0.291	1.082	4.612
		Y- 8	699	5.05	0.269	5.39	0.502	0.489	2.971
		Y- 2	705	2.22	0.837	16.53	0.154	0.021	2.560
		Y- 5	842	6.07	0.776	10.73	0.191	0.457	3.232
		Y- 7	861	2.05	0.855	11.31	0.157	0.095	2.914
		Y- 3	873	3.40	1.118	14.41	0.197	0.274	2.659
		Y-11	874	6.23	0.606	7.77	0.249	0.799	3.818
		Y- 9	903	6.05	0.863	10.38	0.262	0.474	3.322
		Y- 1	1132	4.53	1.596	12.20	0.211	0.493	2.831
		Y- 4	1178	4.97	1.569	11.72	0.229	0.514	2.922
		Y- 6	1309	4.06	1.921	10.99	0.180	0.357	2.701
2	0.82	Y-46	492	2.59	0.380	15.38	0.388	0.570	2.985
		Y-47	716	3.77	0.725	13.85	0.372	0.878	3.716
		Y-48	752	3.96	0.585	11.86	0.273	0.280	2.625
		Y-51	760	4.00	0.865	19.14	0.242	0.125	2.366
		Y-52	798	4.20	1.237	19.04	0.286	0.545	3.142
		Y-49	922	4.85	1.253	14.46	0.236	0.127	2.660
		Y-50	950	5.00	1.128	12.25	0.277	0.852	3.610
		Y-43	998	5.25	1.373	13.52	0.168	-0.009	2.702
		Y-44	1273	6.70	2.274	13.75	0.224	0.169	2.605
		Y-45	1406	7.40	2.602	12.90	0.266	0.549	3.054
3	0.71	Y-19	611	4.08	0.471	12.33	0.224	0.654	3.452
		Y-17	665	5.07	0.610	13.52	0.307	0.958	4.239
		Y-24	716	2.29	0.492	9.40	0.207	0.345	2.955
		Y-25	809	3.73	0.485	7.26	0.258	0.605	3.297
		Y-26	844	4.29	0.604	8.32	0.228	0.907	3.890
		Y-23	946	4.01	0.576	6.29	0.260	0.848	4.189
		Y-27	992	4.82	0.880	13.31	0.273	0.477	2.783
		Y-22	1261	4.32	0.905	11.57	0.290	0.690	2.934
4	0.61	Y-61	408	4.67	0.315	18.50	0.465	0.448	2.927
		Y-55	684	1.89	0.762	15.96	0.174	0.381	0.593
		Y-62	768	5.44	0.666	11.08	0.305	0.762	3.609
		Y-53	787	3.67	0.740	11.72	0.219	0.321	2.847
		Y-56	882	2.89	1.169	14.74	0.219	0.156	2.567
		Y-57	1032	3.96	1.460	13.44	0.222	0.730	3.825
		Y-54	1053	4.69	0.874	7.73	0.281	0.703	3.242
		Y-58	1096	1.99	1.325	10.80	0.232	0.248	3.193
		Y-59	1240	2.54	1.548	9.86	0.246	0.594	2.925
		Y-60	1398	3.48	1.872	9.38	0.261	0.698	3.277
5	0.45	Y-41	511	4.35	0.232	8.70	0.392	0.877	4.079
		Y-31	694	1.95	0.556	11.33	0.197	0.493	2.964
		Y-28	787	3.69	0.303	4.80	0.345	0.599	3.057
		Y-32	802	2.58	0.674	10.27	0.248	0.384	2.841
		Y-29	885	4.44	0.525	6.56	0.254	0.816	3/422
		Y-30	903	4.67	0.601	7.23	0.295	0.300	3.471
		Y-33	910	3.08	0.767	9.07	0.276	0.360	2.770
		Y-42	939	5.28	0.375	4.17	0.355	0.810	3.583
		Y-34	980	3.58	0.920	9.38	0.301	0.595	2.889
		Y-36	1001	1.66	0.758	7.41	0.247	0.245	2.488
		Y-37	1127	2.11	1.072	8.28	0.217	0.224	2.495
		Y-35	1142	4.03	1.136	8.54	0.237	0.454	2.951
		Y-38	1256	2.61	1.148	7.13	0.242	0.508	2.832
		Y-39	1360	3.06	1.216	6.44	0.303	0.532	3.010
		Y-40	1421	3.34	1.307	6.34	0.303	0.742	3.418
6	0.40	Y-66	517	4.48	0.230	8.44	0.289	0.774	3.424
		Y-68	612	2.13	0.388	10.16	0.195	0.748	3.573
		Y-67	714	5.53	0.337	6.47	0.321	0.708	3.269
		Y-71	714	3.80	0.328	6.30	0.260	0.687	3.167
		Y-69	844	3.24	0.549	7.56	0.288	0.639	3.275
		Y-72	977	4.85	0.376	3.86	0.393	0.466	2.802
		Y-63	994	1.74	0.573	5.69	0.253	0.301	2.802
		Y-70	1018	4.27	0.719	6.79	0.260	0.607	3.303
		Y-64	1229	2.50	0.943	6.12	0.239	0.198	2.627
		Y-65	1450	3.47	1.122	5.23	0.293	0.637	3.585
7	0.30	Y-81	483	4.44	0.192	8.08	0.304	0.402	3.228
		Y-75	680	1.87	0.310	6.57	0.254	0.378	2.821
		Y-82	710	5.34	0.263	6.73	0.347	0.470	3.426
		Y-73	720	3.85	0.254	4.80	0.296	0.526	3.189
		Y-76	722	2.95	0.530	9.96	0.242	0.657	3.172
		Y-74	807	4.84	0.358	5.38	0.275	0.651	3.492
		Y-78	846	1.66	0.437	5.99	0.199	0.289	2.612
		Y-77	910	3.91	0.724	8.57	0.285	0.505	2.859
		Y-79	978	2.44	0.570	5.83	0.307	0.299	2.620
		Y-80	1464	3.44	0.830	3.79	0.269	0.440	2.918
8	0.19	Y-86	654	5.23	0.126	2.89	0.440	0.602	3.059
		Y-91	707	3.71	0.106	2.08	0.431	0.531	3.259
		Y-88	724	2.12	0.168	3.14	0.310	0.376	3.063
		Y-87	846	5.51	0.155	2.17	0.429	0.585	3.729
		Y-92	895	4.89	0.160	1.96	0.304	0.817	4.139
		Y-89	906	3.06	0.276	3.29	0.254	0.409	3.067
		Y-83	992	1.63	0.170	1.69	0.385	0.269	2.839
		Y-90	1070	4.26	0.425	1.95	0.425	0.579	3.305
		Y-84	1261	2.64	0.444	2.73	0.331	0.529	3.063
		Y-85	1433	3.39	0.517	2.47	0.335	0.348	2.816
9	0.00	Y-93	811	8.86	0.029	0.43	1.272	0.130	2.676
		Y-94	1322	2.89	0.012	0.07	1.973	0.594	3.891

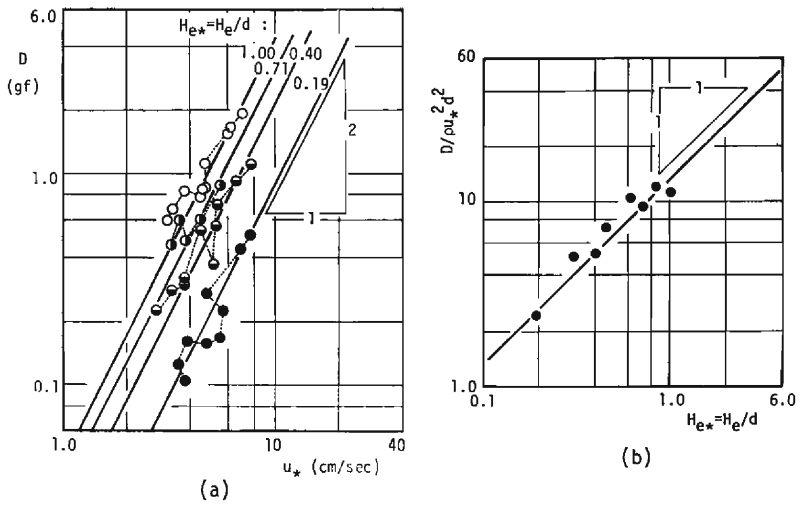

Fig. 4 The relationship between magnitude of drag force and exposure of particle to flow (solitary particle).

a few scatterings, and it is recognized that the linearity constant increases with the exposure of the particle.

In **Fig. 4-(b)**, the relationship between dimensionless drag force defined as $D/\rho u_*^2 d^2$ and relative exposure is indicated and the following empirical expression can be proposed.

$$D/\rho u_*^2 d^2 = 13.5 H_{e*} \qquad (0 < H_{e*} \leqq 1.0) \tag{6}$$

When the testing particle is exposed perfectly to flow, or $H_{e*}=1.0$, the drag coefficient is calculated as

$$C_D = (D/\rho u_*^2 d^2)\,|_{He*=1.0} \cdot (2/A_2 A_*^2) \simeq 0.595 \tag{7}$$

where A_2 is a constant with respect to two dimensional geometrical property of a particle, and A_* is the ratio of the local flow velocity at the center of the particle u to the friction velocity u_*. The value of A_2 is $\pi/4$ in the case of a sphere exposed perfectly to the flow, and the value of A_* becomes 7.6 if the logarithmic law for a velocity profile for rough turbulent regime is applied. The theoretical wall for the logarithmic law is assumed to be $0.2d$ below the top of the particles composing the roughness. The experimentally obtained value of the drag coefficient in the range where the Reynolds number ud/ν is larger than 10^3 is about 0.5~0.7, and it is almost equal or slightly larger than the result of the previous experiment by Coleman[5] which almost coincides with the value for a free falling sphere in still liquid.

By the way, White[11] introduced a packing coefficient η_p to relate the averaged drag force acting upon a sand grain on an erodible bed to friction velocity, and this coefficient was defined as

$$\eta_p \equiv A_2/(D/\rho u_*^2 d^2) \tag{8}$$

The averaged value of η_p is about 0.21 after White[11], and then the value of $(D/$

$\rho u_*^2 d^2$) is about 3. 74. The value of relative exposure corresponding to this magnitude of drag is about 0. 3 according to **Fig. 4-(b)**. This fact gives rise to an estimation that the relative exposure of the particle to be noticed on the consideration of so called critical tractive force is about 0. 3.

On investigation of the mechanism of bed load transport, it is necessary to clarify not only the time-averaged property of drag force inspected above but also its fluctuating characteristics. At first, the variation coefficient of drag force was calculated from the observed data and its result was shown in **Fig. 5**. According to this figure, the systematic change of the variation coefficient of drag α_D is not so appreciable and the averaged value is about constant (0. 2∼0. 4). This value is a little smaller than the one

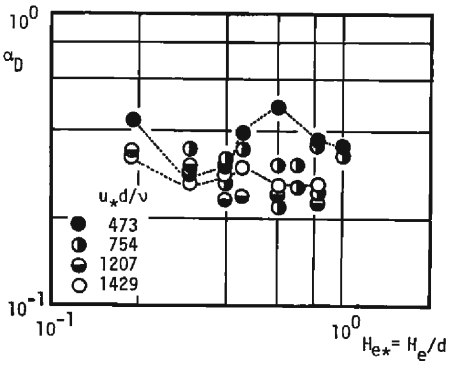

Fig. 5 Variation coefficient of drag force (solitary particle).

estimated from the experimental results on pressure fluctuations near the bed obtained by Chepil[2], Einstein and El-Samni[12] and others, which was quoted to describe the bed load movements by Einstein[13], Paintal[14] and the authors[15] previously. One of the weak points of the authors' measurements explained here is that the sampling interval is too rough for detecting temporal fluctuation, and so more rigorous treatments with respect to fluctuating characteristics may be necessary in the future.

The skewness of fluctuation of drag force is always positive but nearly zero, and its kurtosis is nearly 3. 0 as shown in **Table 1.** Hence, the distribution of drag force may be approximated by Gaussian distribution though it is slightly shifted.

Statistically dynamic properties of fluctuation of drag force are represented by frequency spectrum or autocorrelation function. Some examples of frequency spectra of drag force are shown in **Fig. 6.** According to this figure it is recognized that any spectra are somewhat similar each other. Namely, the following characteristics have been recognized: The spectral density is almost constant in lower frequency range and decreases in proportion to the reciprocal of the frequency in higher frequency range. Furthermore, the examples of temporal autocorrelation coefficients of drag force are shown in **Fig. 7. Fig. 7-(a)** is concerned with the case of perfect exposure and with the Reynolds number as a parameter, while **Fig. 7-(b)** is concerned with

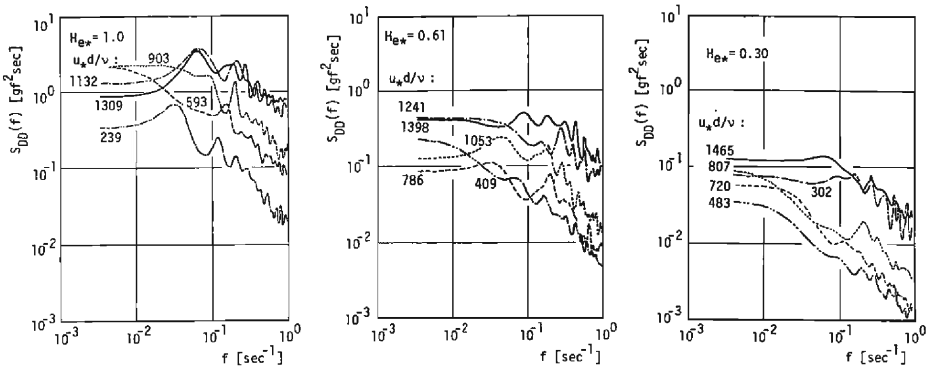

Fig. 6 Frequency spectra of drag force (solitary particle).

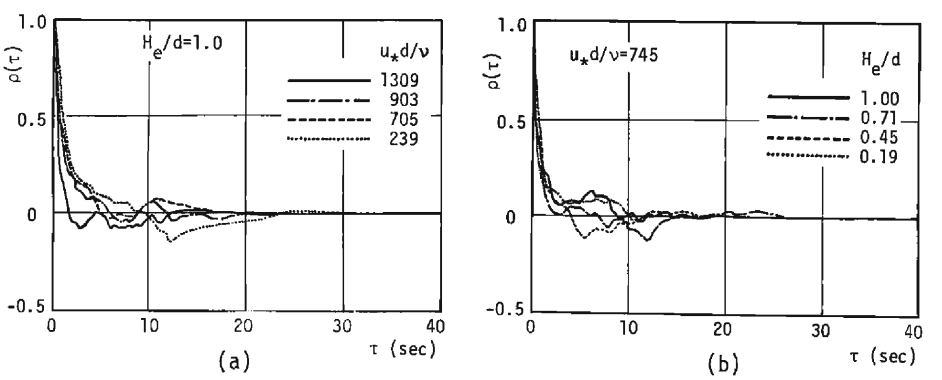

Fig. 7 Temporal autocorrelation coefficients of drag force (solitary particle).

the case of constant Reynolds number and with the relative exposure as a parameter. According to **Fig. 7**-(**a**), the larger the Reynolds number is, the faster the autocorrelation of drag force decays. When the time scale defined as the time period that the autocorrelation coefficient reaches the value $1/e$ ($\simeq 0.37$), or a kind of correlation time, is represented by T_e, the following relation is recognized experimentally between dimensionless correlation time $T_e u_*/d$ and relative flow depth h/d, as shown in **Fig. 8.**

$$T_e u_*/d = 0.3(h/d) \tag{9}$$

Therefore,

$$T_e u_*/h = \text{const.} = 0.3 \tag{10}$$

Moreover, the relaxation distance of spatial correlation of drag force may be estimated as follows.

$$L_e = u \cdot T_e \sim u_* \cdot T_e = 0.3h \tag{11}$$

Hence, L_e may be about twice the flow depth because u/u_* is about 7~8 after the

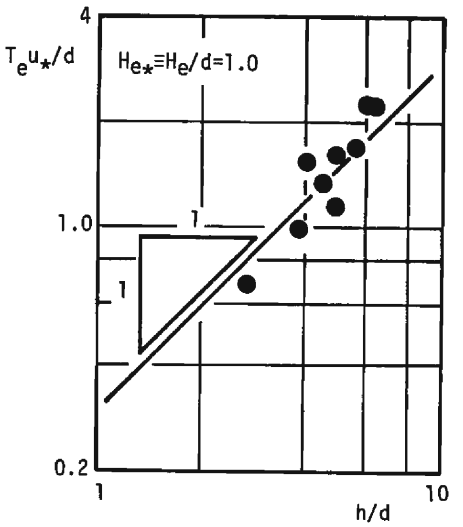

Fig. 8 The relationship between dimensionless correlation time of drag force and relative flow depth.

logarithmic law of flow velocity profile for rough turbulent regime. In other words, the flow depth may be recognized as a spatial scale of the fluctuation of drag force acting upon the bed material particle. On the other hand, **Fig. 7-(b)** indicates that the effect of the exposure of the particle to flow on the time scale or spatial scale of fluctuation of drag force is hardly recognized.

4. Characteristics of Drag Force Acting upon a Particle Influenced by the Surrounding Particles on a Rough Bed

In the case of actual sand bed, the movement of a spherical particle is hindered by the surrounding particles. Therefore, only the knowledge about the hydrodynmic forces acting upon a solitary particle is not enough to describe the actual situation. As a fundamental investigation on such an effect of mutual interference on drag force, some systematic measurements were conducted under simplified conditions.

At first, in the case where two particles separated at interval s in the stream direction were set on a rough bed, the relationship between the drag force acting upon the particle of downstream side and the interval s was inspected. Next, the effect of the number density of surrounding particles on the drag force was investigated.

(1) The Effect of Upstream Side Particle

Another particle was fixed on the rough bed composed of identical glass beads in the closest possible packing, separated at intervel s on the upstream side of the testing particle. Both of the particles were exposed perfectly to flow and the axis connecting

the centers of the two particles was consistent with the direction of the stream. In this experiment, the change of the characteristics of drag force due to the interval of the two particles was investigated. The conditions and the results of the measurements are shown in **Table 2.** Here, the measurements for a solitary particle were also conducted as in the case of $s \to \infty$.

Table 2 Experimental conditions and results (binary particles).

Run No.	u_*d/ν	s/d	D (gf)	$D/\rho u_*^2 d^2$	α_D	Sk	Kr
Z- 1	642	∞	0.924	16.00	0.193	0.045	2.763
Z- 2		0.29	0.305	5.28	0.186	0.224	2.728
Z- 3		1.45	0.560	9.69	0.144	0.054	3.578
Z- 4		3.03	0.639	11.06	0.132	0.132	3.602
Z- 5		4.58	0.845	14.63	0.130	0.194	3.586
Z- 6	884	∞	1.769	16.17	0.226	0.094	2.666
Z- 7		0.29	0.354	3.24	0.292	0.267	3.037
Z- 8		1.45	0.973	8.89	0.161	0.391	4.859
Z- 9		3.03	1.258	11.50	0.153	0.364	3.380
Z-10		4.58	1.317	12.04	0.174	0.175	2.912
Z-11	1005	∞	1.917	13.54	0.286	0.331	2.582
Z-12		0.29	0.393	2.78	0.311	0.357	3.560
Z-13		1.45	1.062	7.50	0.179	0.582	3.966
Z-14		3.03	1.278	9.03	0.187	0.288	3.084
Z-15		4.58	1.632	11.53	0.194	0.066	2.556
Z-16	704	∞	1.052	15.16	0.178	0.001	2.628
Z-17		0.29	0.295	4.25	0.187	0.243	2.903
Z-18		1.45	0.629	9.07	0.119	-0.006	3.797
Z-19		3.03	0.668	9.63	0.116	0.092	4.436
Z-20		4.58	0.796	11.47	0.126	-0.803	4.251
Z-21	895	∞	1.995	17.78	**	**	**
Z-22		0.29	0.275	2.45			
Z-23		1.45	0.885	7.88			
Z-24		3.03	1.101	9.81			
Z-25		4.58	1.307	11.65			
Z-26	514	∞	0.472	12.75	0.207	0.619	4.359
Z-27		0.29	0.082	2.20	0.408	0.071	3.126
Z-28		1.45	0.226	6.11	0.159	0.229	2.642
Z-29		3.03	0.374	10.09	0.136	0.331	3.556
Z-30		4.58	0.403	10.89	0.151	-0.400	5.050

**Fluctuating characteristics have not been analyzed.

In **Fig. 9** the relationship between dimensionless magnitude of drag force $D/\rho u_*^2 d^2$ and dimensionless interval of the two particles s/d is shown. According to this figure, it is concluded that the magnitude of the drag force acting upon the testing particle separated from an upstream side particle at a distance longer than five times the particle diameter is almost same as that for a solitary particle. On the other hand, in the case when the distance between two particles is less than five times the particle diameter, the drag force acting upon the downstream side particle is much influenced by the wake brought about by the upstream side particle. And the following tendency is recognized;

$$D/\rho u_*^2 d^2 \to \begin{cases} 13.5 & (s/d \to \infty) \\ 6.0 \times \sqrt{s/d} & (s/d \to 0) \end{cases} \tag{12}$$

Using the method of data correlation proposed by Churchill and Usagi[16], the following equation which is adaptable to the whole range of s/d can be proposed.

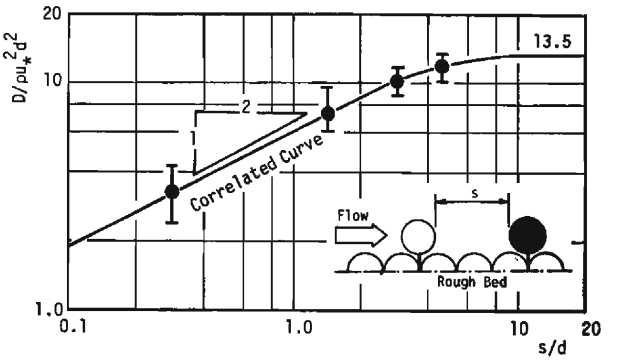

Fig. 9 The relationship between dimensionless magnitude of drag force and dimensionless interval of two particles.

$$D/\rho u_*^2 d^2 = [(s/d)^{4.5}/\{10^{-7}+6.7\times10^{-11}(s/d)^{4.5}\}]^{1/9} \quad (13)$$

Next, the characteristics of fluctuation of drag force under such a condition were investigated. The variation coefficient of drag force is shown in **Table 2** and it is recognized that, the shorter the distance of the two particles is, the larger the variation coefficient becomes, and that the value of the variation coefficient may increase with the Reynolds number. Such an increase of variation coefficient may be caused by the effect of the wake induced by the upstream side particle.

Furthermore, some examples of frequency spectra of drag force under this condition are shown in **Fig. 10**, and their shapes are hardly converted from those for a solitary particle shown in **Fig. 6**.

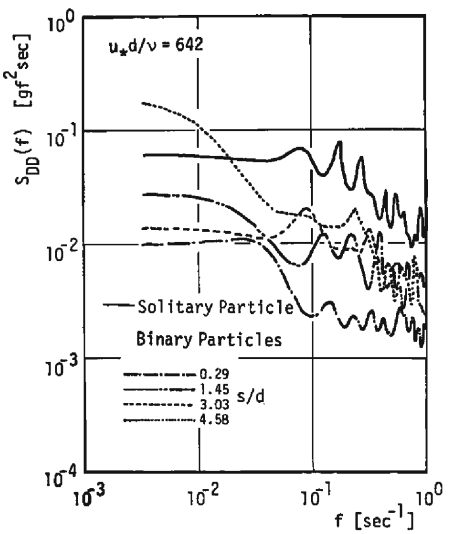

Fig. 10 Frequency spectra of drag force (binary particles).

(2) The Effect of Number Density of Particles on a Rough Bed

Next, the effect of number density of particles on a rough bed for drag force acting upon a noticed particles among them was investigated by several measurements. The bed was the same as one used in the preceding measurements, and some identical glass beads were fixed on this rough bed employing several spacings in a hexagonal pattern. The experimental conditions and the results are shown in **Table 3.**

Table 3 Experimental conditions and results (distributed particles).

Run No.	n_*	u_*d/ν	D(gf)	$D/\rho u_*^2 d^2$	α_D	Sk	Kr
W- 1	0.137	817	0.386	3.94	0.177	0.381	3.290
W- 2		1088	0.558	3.21	0.238	0.737	3.517
W- 3		1235	0.691	3.08	0.292	0.674	3.298
W- 4		695	0.356	5.01	0.173	0.461	3.281
W- 5		977	0.342	2.44	0.282	0.918	4.761
W- 6		1154	0.533	2.72	0.261	0.825	4.541
W- 7		675	0.301	4.51	0.191	0.423	3.303
W- 9	0.080	839	0.449	4.34	0.303	-0.366	3.097
W-10		1053	0.524	3.22	0.278	0.293	4.026
W-11		656	0.328	5.20	0.153	-0.025	3.652
W-12		858	0.440	4.07	0.176	0.460	3.834
W-13		1050	0.522	3.22	0.194	0.604	3.805
W-14		739	0.298	3.71	0.221	0.060	2.930
W-15		961	1.175	8.66	0.161	0.387	3.365
W-24	0.035	524	0.532	13.18	0.123	0.084	3.582
W-25		752	0.806	9.70	0.168	0.361	3.573
W-26		592	0.402	7.80	0.145	0.257	3.417
W-27		839	0.852	8.25	0.183	0.374	3.207
W-28		1036	1.383	8.78	0.194	0.448	3.361
W-29		675	0.530	7.93	0.157	0.215	3.330
W-30		909	0.910	7.50	0.189	0.281	2.846
W-31		1088	1.220	7.02	0.221	0.697	3.544
W-32	0.054	720	0.527	6.91	0.144	0.154	3.264
W-33		933	0.757	5.92	0.198	0.392	3.511
W-34		1126	1.121	6.02	0.205	0.565	3.554
W-35		602	0.479	9.01	0.134	0.203	3.374
W-36		831	0.756	7.45	0.189	0.341	3.445
W-37		1040	0.963	6.06	0.213	0.430	2.801
W-38		575	0.334	6.88	0.167	0.364	3.096
W-39		803	0.669	7.07	0.183	0.458	3.221

At first, the relationship between the time-averaged magnitude of drag force D and the friction velocity u_* was investigated. The obtained experimental data are shown in **Fig. 11**-(**a**), where dimensionless number density n_* defined by the following equation is indicated as a parameter.

$$n_* = \nu_s \cdot A_2 d^2 \tag{14}$$

where ν_s is the number density of particles on a rough bed and is the number of particles per unit area of the bed. According to **Fig. 11**-(**a**), it is recognized that D is proportional to u_*^2 and that, the larger the number density is, the smaller the linearity constant becomes. The relationship between the dimensionless drag force $D/\rho u_*^2 d^2$ and n_* is shown in **Fig. 11**-(**b**), which is obtained from **Fig. 11**-(**a**). If $n_* \to 0$, $D/\rho u_*^2 d^2$ tends to 13.5 which is the value in the case of a perfectly exposed solitary particle. If n_* becomes larger, $D/\rho u_*^2 d^2$ is inversely proportional to n_*. These results can be arranged to the following expression by making use of a kind of data correlation

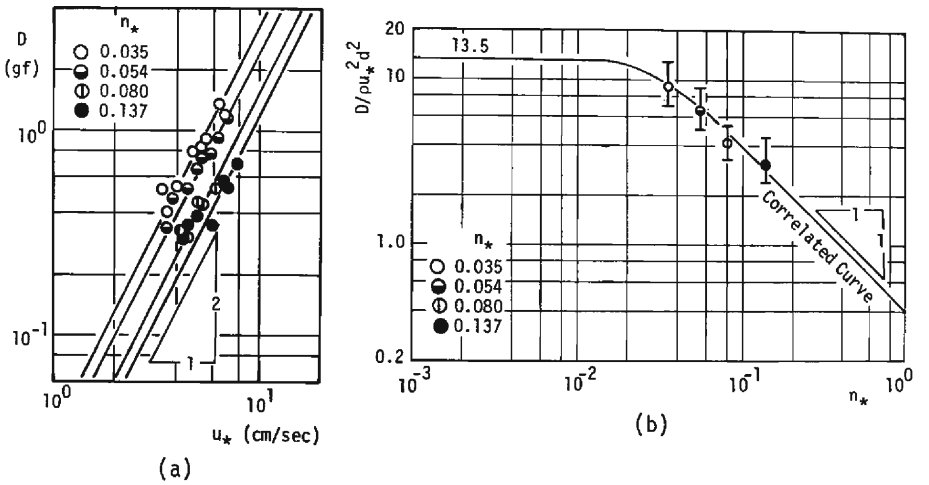

Fig. 11 The relationship between magnitude of drag force and number density of particles distributing on rough bed.

method proposed by Churchill and Usagi[16].

$$D/\rho u_*^2 d^2 = (0.0004 + 15.6 n_*^3)^{-3} \tag{15}$$

Next, the statistical properties of the fluctuations of drag force acting upon a testing particle under this condition were investigated. In **Fig. 12**, the relationship between the variation coefficient of drag force α_D and the number density of particles on a rough bed or the particle Reynolds number is shown. The dimensionless number density n_* is indicated as a parameter in this figure. According to this figure, α_D may increase with the Reynolds number, and it may be larger when n_* is large. In addition to them, spectral characteristics were also inspected under this condition, but appreciable differences from those obtained in the preceding parts of this paper were hardly recognized.

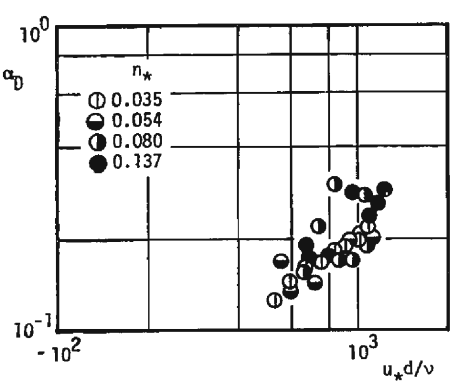

Fig. 12 Variation coefficient of drag force (distribution particles).

5. Conclusions

In this paper, the results of direct measurements of drag force acting upon a spherical particle near a rough bed under several conditions were explained. Particularly, the effects of relative exposure of a particle to flow and of interference of surrounding particles on the characteristics of drag force were investigated, and the obtained results must be useful to researches of the mechanics of bed load transport, though further inspections or recognitions of the experimental results must be necessary.

In this study, equipment for dynamical measurement of drag force was devised by making use of some strain gauges and a strain-meter. This device made it possible to measure hydrodynamic drag force acting upon a particle resting on the bed under some defined conditions.

In the following, the main results of this paper will be summarized. First, the mean drag coefficient of a particle perfectly exposed to flow on a rough bed is about 0.5～0.7 according to the measurement and it is almost equal or silghtly larger than the value for a free falling sphere in still liquid which has been adopted in analysis of bed load motion by several researchers without any confidence.

As for the fluctuating characteristics of hydrodynamic force acting upon a particle near a bed, the fluctuation of drag force can be approximated by a Gaussian process and, by inspecting its autocorrelation, the characteristic longitudinal scale of its fluctuation is expected to be about twice the flow depth.

Next, the influence of exposure of a particle on a bed upon the magnitude of drag force was investigated, and the relationship between a dimensionless magnitude of drag force and the relative exposure was clarified experimentally. As a result, the magnitude of drag force may be proportional to the relative exposure.

The interfering effects of surrounding particles were investigated by the dynamical measurements of drag force conducted under two kinds of specialized conditions. In one case two particles were fixed at various intervals on a rough bed in the flow direction, and in the other case some particles were fixed in a hexagonal pattern by several kinds of number density of perfectly exposed particles on a rough ded. These experiments gave us the following two relationships. One is the relationship between the magnitude of drag force and the interval of two particles in the flow direction, and the other is between the magnitude of drag force and the number density of exposed particles on a rough bed. According to these experimental results, the following was recognized. In the case that the distance between the two particles is smaller than five times the particle's diameter, a particle in the upstream side has an appreciable effect on the drag force acting upon the particle in dowestream side and the magnitude of drag force is proportional to the square root of the distance of the two particles. On the other hand, the magnitude of drag force is affected by surrounding particles in the case that the dimensionless number density $n_*(\equiv \nu_g A_2 d^2)$ is larger than 2×10^{-2} and it is almost inversely proportional to the number density of perfectly exposed particles on a rough bed.

As mentioned above, the variation of the magnitude of drag force due to some idealized changes of conditions was clarified, and it may be possible to formulate the magnitude of drag force acting upon a bed material particle under several conditions more conformable with actual sand beds.

The results obtained by this study may be significant or instructive, but further subsequent investigations must be necessary to apply them to some problems of alluvial processes. The following three are particularly important, and we are now in preparation of them. One is to combine the effect of exposure and that of interference by surrounding particles and to verify a combined model experimentally. Another is to formulate the statistical properties of fluctuating hydrodynamic forces. And the other is simultaneous measurement of drag and lift. Clarifying these problems must make great progress in the study of the mechanics of bed load transport.

Acknowledgement

Sincere gratitude is expressed to Mr. Yasuhiro Hosokawa (M. Eng., Ministry of Transportation) and Mr. Shogo Murakami (M. Eng., Japan Overseas Cooperation Volunteers) for their helps in carrying out the experiments and the exhaustive data processings.

References

1) Chepil, W. S.: The Use of Evenly Spaced Hemispheres to Evaluate Aerodynamic Forces on a Soil Surface. Trans. A. G. U., Vol. 39, No. 3, pp. 397-404, 1958.
2) Chepil, W. S.: Equilibrium of Soil Grains at Threshold of Movement by Wind. Soil Science Society Proceedings, Vol. 23, No. 6, pp. 422-428, 1959.
3) Chepil, W. S.: The Use of Spheres to Measure Lift and Drag on Wind Eroded Soil Grains. Soil Science Soceity Proceedings, Vol. 25, pp. 343-345, 1961.
4) Coleman, N. L.: A Theoretical and Experimental Study of Drag and Lift Forces Acting on a Sphere Resting on a Hypothetical Stream Bed. Proc. XIIth Congress, IAHR, Fort Colorad, USA, Vol. 3, Paper C-22, pp. 185-192, 1967.
5) Coleman, N. L.: The Drag Coefficient of a Stationary Sphere on a Boundary of Similar Spheres. La Houille Blanche, No. 1, pp. 17-21, 1972.
6) Aksoy, S.: Fluid Force Acting on a Sphere near a Solid Boundary. Proc. XVth Congress, IAHR, Istanbul, Turkey, Vol. 1, Paper A-29, pp. 217-224, 1973.
7) Davies, T. R. H. and M. F. A. Samad: Fluid Dynamic Lift on a Bed Particle. Proc. ASCE, Journal of the Hydraulics Division, Vol. 104, HY 8, pp. 1171-1182, 1978.
8) Garde, R. J. and S. Sethuraman: Variation of the Drag Coefficient of a Sphere Rolling along a Boundary. La Houille Blanche, No. 7, pp. 727-732, 1969.
9) Bagnold, R. A.: Fluid Forces on a Body in Shear-Flow: Experimental Use of 'Stationary Flow.' Proc. Royal Society of London, A-340, pp. 147-171, 1974.
10) Coleman, N. L.: Bed Particle Reynolds Modelling for Fluid Drag. Journal of Hydraulic Research, IAHR, Vol. 17, No. 2, pp. 91-105, 1979.
11) White, C. M.: The Equilibrium of Grains on the Bed of a Stream. Proc. Royal Society of London, A-174, pp. 324-334, 1940.
12) Einstein, H. A. and E. A. El-Samni: Hydrodynamic Forces on a Rough Wall. Review of Modern Physics, 21, pp. 520-524, 1949.
13) Einstein, H. A.: The Bed Load Function for Sediment Transportation in Open Channel

Flows. Technical Bulletin, Soil Conservation Service, U. S. Department of Agriculture, No. 1026, 78p., 1950.
14) Paintal, A. S.: Stochastic Model of Bed Load Transport. Journal of Hydraulic Research, IAHR, Vol. 9, No. 4, pp. 527-554, 1971.
15) Nakagawa, H. and T. Tsujimoto: On Probabilistic Characteristics of Motion of Individual Sediment Particles on Stream Beds. Proc. 2nd International IAHR Symposium on Stochastic Hydraulics, Lund, Sweden, Reprinted in the book "Hydraulic Problems Solved by Stochastic Methods", pp. 293-316, 1976.
16) Churchill, S. W. and R. Usagi: A Standarzation Procedure for the Prediction of Correlation in the Form of a Common Empirical Equation. Industrial Chemistry, Fundam., Vol. 13, No. 1, pp. 39-44, 1974.

Notations

A_2	Two dimensional geometrical constant for particle $(=\pi/4)$
A_*	$=u/u_*$
C_D	Drag coefficient
C_{DV}	Calibration constant of measuring equipment
D	Magnitude of drag force
d	Particle diameter
Fr	Froude number of flow
f	Frequency
f_0	Characteristic frequency of measuring equipment
$H(f)$	Response function of measuring equipment
H_e	Exposure of testing particle to flow
H_{e*}	Relative exposure of particle $(=H_e/d)$
h	Flow depth
I_e	Energy gradient of flow
i_b	Bed slope
i_w	Water surface slope
Kr	Kurtosis of fluctuating drag force
k	Spring constant of acrylic rod of measuring equipment
L_e	Relaxation distance of spatial correlation of drag force
M	Virtual mass of particle
n_*	Dimensionless number density of particles on rough bed $(=\nu_s A_2 d^2)$
$P_{DD}(f)$	Power spectral density function of drag force
$P_{VV}(f)$	Power spectral density function of out-put of measuring equipment
Sk	Skewness of fluctuating drag force
s	Interval of two particles
T_e	Relaxation time of temporal autocorrelation of drag force
u	Local flow velocity at the center of the particle
u_*	Friction velocity of flow
α_D	Variation coefficient of fluctuating drag force
ν	Kinematic viscosity of fluid
ν_s	Number density of particles on rough bed
ρ	Density of fluid
η_p	Packing coefficient introduced by White